

A. S. Ivashutenko, I. V. Ionov, A. S. Maznoy, A. A. Sivkov and A. A. Solovyev*

Comparative Evaluation of Spark Plasma and Conventional Sintering of NiO/YSZ Layers for Metal-Supported Solid Oxide Fuel Cells

DOI 10.1515/htmp-2016-0193

Received September 6, 2016; accepted March 1, 2017

Abstract: NiO/YSZ anode layers for metal-supported solid oxide fuel cells (MS-SOFCs) were fabricated by spark plasma sintering (SPS). SPS parameters were optimized in order to achieve anodes of the desired microstructure. The effect of sintering conditions on microstructure of NiO/YSZ was studied by scanning electron microscopy and X-ray diffractometry. Also NiO/YSZ layers were formed on porous metal supports by a screen-printing method and sintered in inert atmosphere and vacuum by conventional sintering technique. At temperatures above 1,200 °C in inert atmosphere and vacuum nickel oxide dissociation and its massive agglomeration are observed during conventional sintering. SPS process allows sintering of NiO/YSZ granules without NiO dissociation, Ni agglomeration and the metal substrate oxidation at 1,100 °C. SPS sintered anodes demonstrate sufficiently homogeneous distribution of NiO and YSZ making a conduction path for electrons and ions. Well-bonded metal support/anode interface was obtained.

Keywords: solid oxide fuel cell, spark plasma sintering, anode, cermet, microstructure

PACS® (2010). 81.20.Ev

Introduction

Solid oxide fuel cells (SOFC) involve many benefits over the conventional ways of generating power such as high density of energy, large efficiency, environmental friendliness, simultaneous generation of heat and electricity, as well as fuel flexibility. Metal-supported solid oxide fuel cells have many advantages as compared to electrode or electrolyte-supported fuel cells [1]. This is related to higher thermal conductivity and plasticity of the metal substrate, which enhances the SOFC thermal stability and reduces internal temperature gradients capable of damaging ceramic layers. The performance of each SOFC component is critically dependent on its microstructure. For example, the microstructure of the anode is a key factor for controlling fuel transport, oxidation, and electrical conductivity [2]. Generally, the porosity of the anode should be about 25–35 % in order to avoid strong concentration polarization. A continuous network structure of both Ni and YSZ, high triple-phase boundary (TPB) length and good adherence to the other SOFC layers are also required.

The microstructure of NiO/YSZ anode is mainly determined by processing methods. The composition of the SOFC anode, particle sizes of the powders and the manufacturing method are important to achieving high electronic and ionic conductivity, high activity for electrochemical reactions. Researchers have employed a variety of manufacturing techniques to fabricate SOFC anodes. Among them, powder methods, such as tape casting [3], screen-printing [4], atmospheric plasma spraying [5], as well as vacuum deposition methods including magnetron sputtering [6] and pulsed laser deposition [7] are widely used for this purpose. However, not all of these methods are suitable for the manufacture of metal-supported solid oxide fuel cells. All powder methods require high sintering temperatures (normally, 1,200–1,450 °C) of deposited layers. Jiang [8] showed

*Corresponding author: **A. A. Solovyev**, Department of Experimental Physics, National Research Tomsk Polytechnic University, 30 Lenin Avenue, Tomsk, Russia 634050; Institute of High Current Electronics, Siberian Branch, Russian Academy of Sciences, 2/3 Akademicheskoy Avenue, Tomsk, Russia 634055, E-mail: andrewsol@mail.ru
<http://orcid.org/0000-0001-7775-9769>

A. S. Ivashutenko, Department of electrical supply of industrial enterprises, National Research Tomsk Polytechnic University, 30 Lenin Avenue, Tomsk, Russia 634050, E-mail: ivashutenko@mail.ru

I. V. Ionov, Laboratory of Heat and Mass Transfer Problems in Plasma Processes and Hydrogen Fuel Cells, National Research Tomsk Polytechnic University, 30 Lenin Avenue, Tomsk, Russia 634050; Institute of High Current Electronics, Siberian Branch, Russian Academy of Sciences, 2/3 Akademicheskoy Avenue, Tomsk, Russia 634055, E-mail: ionovigor@gmail.com

A. S. Maznoy, Tomsk Scientific Center SB RAS, Akademicheskoy Av., 10/4, Tomsk 634055, Russia, E-mail: maznoy_a@mail.ru

A. A. Sivkov, Department of electrical supply of industrial enterprises, National Research Tomsk Polytechnic University, 30 Lenin Avenue, Tomsk, Russia 634050, E-mail: sivkovaa@mail.ru

that the lowest electrode ohmic and polarization resistance was observed for Ni/8YSZ cermet anodes sintered at 1,400 °C. High sintering temperature is essential to create a rigid YSZ structure to support the Ni phase and the formation of Ni-to-Ni electronic contact network [9]. The sintering at a high temperature could lead to oxidation of the metal support and the shrinkage of porous metal substrate may occur. High temperature sintering is a time-consuming process and will inevitably introduce many defects due to atomic interdiffusion. Also dissociation of nickel oxide at temperature about 1,230 °C takes place if sintering is not carried out in an air atmosphere. Dissociation degree of NiO phase depends not only on the temperature but also the holding time at this temperature. Dissociation of nickel oxide during sintering process is undesirable, because it leads to agglomeration of Ni particles in the anode. Metallic nickel has a lower melting point than nickel oxide: 1,455 °C for Ni versus 1,984 °C for NiO. This means that metallic nickel is more likely to undergo agglomeration which resulting in a loss of structural homogeneity of the anode. Therefore high temperature sintering is not suitable for the manufacture of metal-supported solid oxide fuel cells.

Hence, there are a limited number of techniques for forming electrode and electrolyte layers for metal-supported SOFC such as vacuum plasma spray [10], atmospheric plasma spray [11], and high-temperature sintering in a reducing atmosphere [12]. Spark plasma sintering (SPS) technique has already been demonstrated as a method to fabricate various SOFC components, mainly electrolyte [13-15]. Typical sintering time can be reduced from 12 h for conventional sintering, using an electric resistance furnace, to approximately 30 min with the use of the SPS technique [13]. Spark plasma sintering simultaneously applies pulsed electrical current and pressure directly on the sample leading to densification at relatively lower temperatures and short retention times. High heating rates of samples (hundreds of °C min⁻¹) can be achieved and densifying mechanisms like surface diffusion can be surpassed [14]. The heating power is not only distributed over the volume of the powder compact homogeneously, but moreover the heating power is dissipated exactly at the locations where energy is required for the sintering process, namely at the contact points of the powder particles.

Although SPS technique is mainly used for electrolytes manufacturing, Weng et al. [16] described fabrication of highly conductive Ni/YSZ cermet via SPS in vacuum at 1,100 °C for 1 min under pressure of 100 MPa. The cermet density was about 96 %, which is too high for anodes. But, the optimization of SPS of Ni/YSZ was not the main goal of that study. Yoo et al. [17] reported fabrication of Ni/YSZ

anode supports by high-frequency induction heated sintering (HFIHS). This sintering method is similar to SPS. Researchers performed sintering at 1,100–1,200 °C for 3 min under different uniaxial pressures at a 133 Pa vacuum. The porosity of the 60 vol.% Ni/YSZ cermet was 24–28 % depending on the size of the powder particles and did not depend on pressure during the sintering process. The samples sintered by HFIHS show higher strength and electrical conductivity than conventionally sintered samples due to uniform pore and grain distribution and better Ni particle-to-particle contact.

Thus, SPS technique seems to be a promising tool for fabrication of SOFC anodes. However, to the best of our knowledge, there are no studies devoted to fabrication of NiO/YSZ anode layers on metal supports by SPS. In this study, we attempted to form NiO-YSZ layers on Ni-Al substrates via SPS and conventional sintering in inert atmosphere and vacuum to obtain NiO-YSZ layers with desired microstructure and without oxidation of metal support.

Experimental

The starting materials for SPS synthesis were powders of 8 mol.% Y₂O₃-stabilized zirconia (YSZ) zirconium (specific surface area – 5–7 m²/g, particle size distribution d₅₀ = 0.5–1.0 μm) and NiO (specific surface area – 2–4 m²/g, particle size distribution d₅₀ = 0.5–1.0 μm) supplied by CERA-FC Co., Ltd., Korea. The NiO and YSZ powders were mixed for 2 h in 8,000 M Mixer/Mill planetary mill (SPEX Sample Prep.). The composite 50 vol.% NiO/YSZ was prepared. Also the NiO/YSZ anode layer was formed with the use of a screen-printing paste composed of NiO (50 %)/ZrO₂:Y₂O₃(50 %) and produced by ESL Electroscience, USA. Ni-16 mass% Al porous substrates with diameter of 20 mm and thickness of 2 mm were produced by self-propagating high-temperature synthesis also known as combustion synthesis. Detailed description of the method is presented in [18].

The mixture of NiO and YSZ powders was sintered in SPS10-4 apparatus (Advanced Technology, USA) using a graphite die with a diameter of 20 mm. The SPS synthesis was carried out in Ar at 1,100 °C and the holding time was 1, 5 and 10 min. High-purity argon (purity 99.998 %; oxygen content is 0.0002 %) was used during the sintering. The heating rate was 50 °C min⁻¹ under a pressure of 10–15 MPa. Temperature monitoring was carried out using the K-type thermocouple, placed in the closed hole of the lower punch in 2.5 mm from the powder. The cooling rate from the sintering temperature was 500 °C min⁻¹. Pressure was applied at the beginning of the sintering process and was

removed after complete cooling of the sample. After sintering of the NiO/YSZ layer, the surface of the anode was polished to remove graphite paper. The final thickness of NiO/YSZ layer was 600 μm .

Screen-printed NiO/YSZ anodes with 60 μm thickness were sintered in Ar atmosphere at a temperature of 1,250 °C and in the vacuum furnace at a temperature of 1,200 °C (residual pressure of $1.33 \cdot 10^{-3}$ Pa). In the first case, vacuum furnace VHT 8/22GR (Nabertherm, Germany) with graphite felt insulation was used. In the second case, vacuum furnace SNVE-16/13 (Prisma, Russia) was used. Time of isothermal holding at the maximum temperature in all cases was 2 h. The sintering temperature was selected in the range of 1,200–1,250 °C for the following reasons: (a) at a lower temperature sintering of YSZ granules will be insufficient, (b) at a higher temperature the maximum exploitation temperature of the Ni–16 mass% Al substrates will be exceeded (it is equal to 1,250 °C) and considerable shrinkage of Ni-Al substrates will be observed.

The phase composition of the products was determined by XRD analysis (Shimadzu 7000S). The XRD profiles were recorded using monochromatized Cu-K α radiation. Morphology and grain size of sintered products were studied using scanning electron microscopy (SEM – 515 “Philips” and SEM Hitachi TM3000). The chemical composition was determined by micro X-ray spectrum analysis (energy-dispersive X-ray spectroscopy – EDS) at the Camebax Micro-Beam device. Surface porosity values were obtained from the SEM images that were imported into the Image-J software.

Results

Conventional sintering of NiO/YSZ

Our results showed that conventional sintering of NiO/YSZ in Ar and vacuum at temperatures of 1,200–1,250 °C led to NiO decomposition. This heat treatment modified the color of anode layer from green to gray indicating a change of chemical composition. NiO reduction during sintering in Ar is apparently caused by the high content of carbon in a vacuum furnace, resulting from the use of graphite felt insulation. NiO reduction during vacuum sintering is caused by the low oxygen partial pressure in the chamber. Taking into account that air contains about 20% of oxygen, the oxygen partial pressure under a residual pressure of $1.3 \cdot 10^{-3}$ Pa in the furnace was about $0.266 \cdot 10^{-3}$ Pa. This is almost 10 times less than the NiO dissociation pressure at 1,200 °C (about $3 \cdot 10^{-3}$ Pa) [19].

Figure 1 shows typical X-ray diffractogram of NiO/YSZ layer sintered in vacuum at a temperature of 1,200 °C and a residual pressure of $1.33 \cdot 10^{-3}$ Pa. There is no nickel oxide phase in the sample containing only pure nickel phase and YSZ.

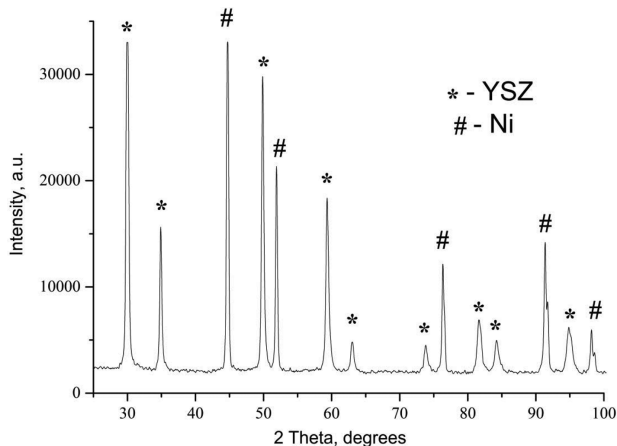


Figure 1: X-ray diffractogram of NiO/YSZ layer sintered in vacuum at a temperature of 1,200 °C and a residual pressure of $1.33 \cdot 10^{-3}$ Pa.

The scanning electron microscopy demonstrated that both NiO/YSZ layers sintered in Ar atmosphere and vacuum at temperatures of 1,200–1,250 °C have inhomogeneous structure (Figure 2). The structure contains many large Ni granules surrounded by the voids both on the surface and in the volume of the layer.

The chemical composition of these granules was determined by micro X-ray spectrum analysis (Figure 3). The growth of large Ni grains occurs due to merging of small-sized grains and is associated with the minimization of the surface free energy. Voids are formed in place of small-sized Ni grains. Ni agglomerates have length from 1 to 6 μm after sintering in Ar atmosphere and about 2–8 μm after sintering in vacuum. In both cases porosity of layers obtained by Image-J analysis is relatively high and equal to 39–41%. The porosity was analyzed with the assumption that the porosity on the surface is equivalent to the overall layer porosity.

Spark plasma sintering of NiO/YSZ

According to the XRD pattern of the NiO and YSZ powders mixture, a pure crystalline state of YSZ and NiO with a cubic structure is observed (Figure 4, curve 1). In addition, the XRD patterns revealed the absence of extra reflections belonging to any additional phase in the

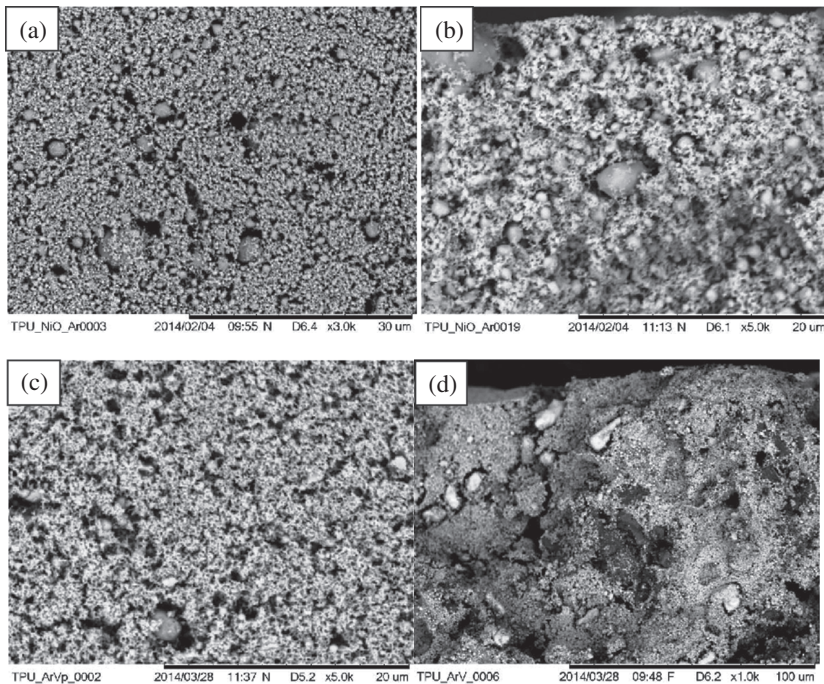


Figure 2: The NiO-YSZ layers surface (a, c) and cross-section (b, d) after sintering at a temperature of 1,250 °C in an argon atmosphere (a, b) and a temperature of 1,200 °C in vacuum at a residual pressure of $1.33 \cdot 10^{-3}$ Pa (c, d) for 2 h.

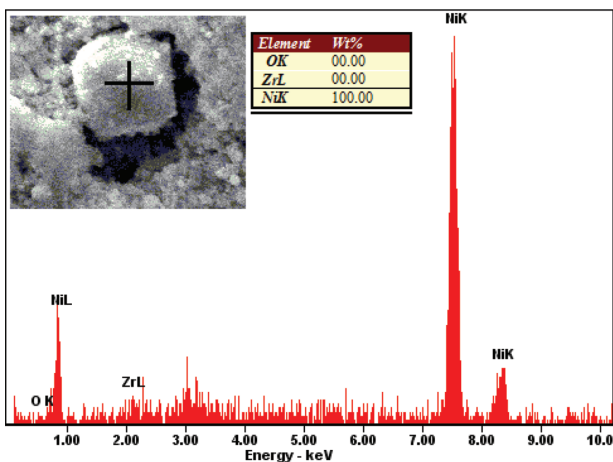


Figure 3: EDS spectra of large Ni grain observed in the NiO-YSZ layer sintered in vacuum at temperature of 1,200 °C.

powder. XRD pattern of NiO-YSZ layer fabricated by spark plasma sintering in Ar at 1,100 °C for 1 min (pressure is 10 MPa) showed that there is no NiO decomposition during SPS. Nickel phase is not detected. As well, sample did not change its color after sintering. This is due to the small holding time at high temperature.

In work of Bezdorozhev et al. [20] NiO was found to be reduced to the metallic state after SPS of NiO/YSZ powders. The sintering was performed in a vacuum atmosphere at 950–1,100 °C for 1–10 min under a constant pressure of 15 MPa (30–50 wt.% flour was added into NiO/YSZ powder as a pore-forming agent). The reduction of NiO was also observed for NiO/YSZ SPSed at 1,100 °C

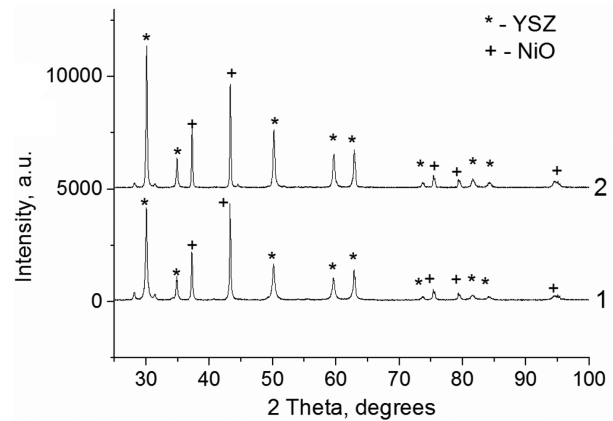


Figure 4: X-ray diffractograms: 1 – NiO/YSZ powder mixture, 2 – NiO/YSZ layer fabricated by spark plasma sintering in Ar at 1,100 °C for 1 min (pressure is 10 MPa).

for 1 min under a pressure of 100 MPa in the study by Weng et al. [16]. The source of reduction atmosphere in this case, apparently, is carbon from flour, which performs the function of pore-former and reducing agent at the same time.

Figure 5 shows the microstructure of NiO/YSZ sample sintered by SPS in Ar at 1,100 °C for 1 min (pressure is 10 MPa). The structure consists of irregularly shaped granules with a size of 0.2–2 μm, which are poorly bonded to each other.

To improve connectivity of granules the samples were sintered by SPS in Ar at 1,100 °C with a larger holding time (5 and 10 min) and pressure of 15 MPa.

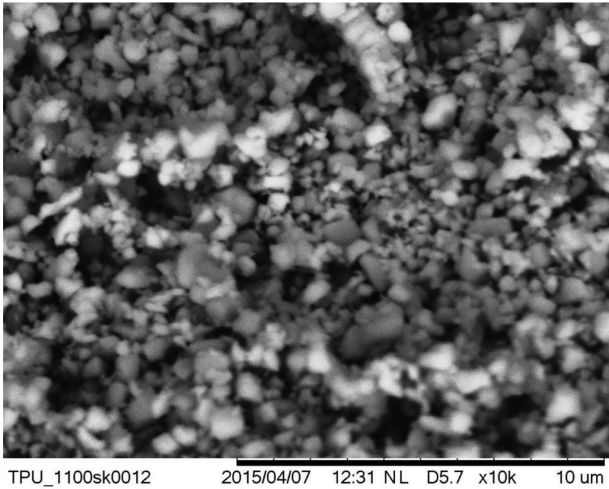


Figure 5: SEM micrograph of surface of NiO-YSZ layer sintered by SPS in Ar at 1,100 °C for 1 min (pressure is 10 MPa).

The reduction of NiO was not observed also. It is clear from Figure 6 that fine pores are uniformly distributed, and the network structures of NiO and YSZ are well built up with good connectivity. Meanwhile, there is no appreciable difference in microstructure at holding times 5 and 10 min. The samples show similar values of apparent porosity (about 49–50%) across the range of used holding times during sintering. From Figure 6, it also can be seen that anode and Ni-Al support has very good contact with each other.

Sample sintered by SPS with a holding time 10 min was maintained in hydrogen at 800 °C for 2 h to Ni reduction. The SEM images, which are taken on the surface, and the cross section of the sample after reduction are shown in Figure 7.

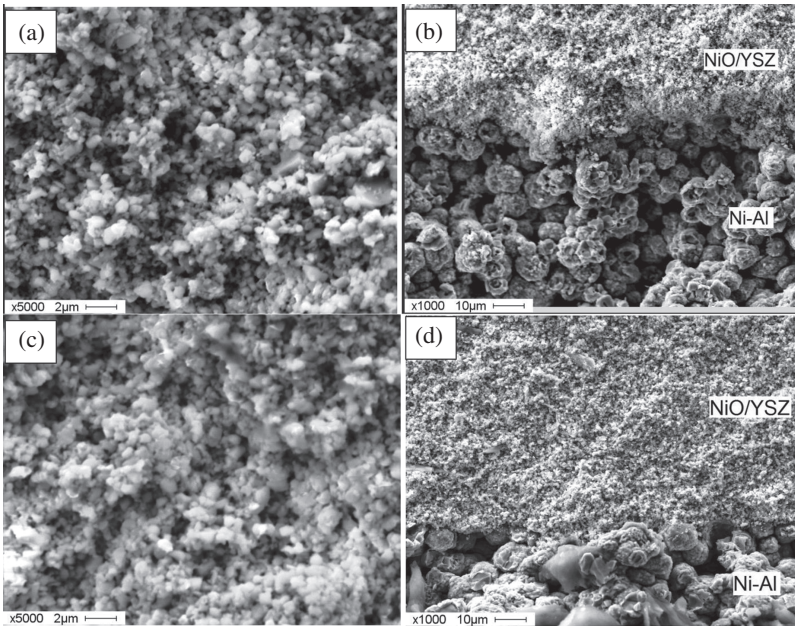


Figure 6: The surface (a, c) and cross-section (b, d) of NiO-YSZ layers after sintering by SPS in Ar at 1,100 °C for 5 min (a, b) and for 10 min (c, d). Pressure is 15 MPa.

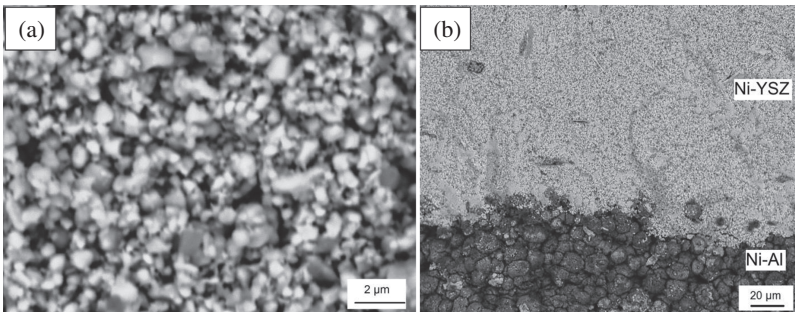


Figure 7: The surface (a) and cross-section (b) of NiO-YSZ layers after sintering by SPS in Ar at 1,100 °C for 10 min and reduction in hydrogen at 800 °C for 2 h.

From Figure 7, it can be seen that the anode has a homogeneous distribution of Ni and YSZ granules along the cross-section and growth of large Ni granules does not occur, unlike the method of conventional sintering. Grain size is not increased and is in the range of approximately 0.2–2 μm. Good bonding between anode and Ni-Al support will result in efficient electrons transport from the anode to current collector. It is important to note that SPS under pressure is an effective way to avoid warping of Ni-Al + NiO/YSZ bilayers due to the difference in sintering kinetics, thermal expansion coefficient mismatch, or density variations [21].

Conclusion

The spark plasma sintering technique has been successfully applied for fabrication of Ni-Al + NiO/YSZ bilayers for metal-supported solid oxide fuel cells. NiO/YSZ layers with the desired porosity can be effectively fabricated by SPS technique with a significantly short sintering time (5–10 min) compared with conventional sintering (2 h) in an electrical resistance furnace. Conventional sintering of NiO/YSZ in Ar atmosphere and in the vacuum leads to NiO reduction and formation of massive Ni agglomerates that break down the microstructural uniformity of the anode layer. Spark plasma sintering can reduce the sintering temperature of NiO/YSZ up to 1,100 °C. Reduction of NiO does not happen during SPS process. The microstructure of the anode was shown to be sufficiently controllable by SPS consolidation parameters. The final porosities of the samples sintered at 1,100 °C do not significantly change with varying sintering time from 1 to 10 min. An anode layer with the desired microstructure is consolidated at a minimum pressure of 15 MPa and a minimum holding time of 5 min. A layer with relatively high porosity (about 50%), sufficient for effective fuel gas transport, can be fabricated without the use of a pore-former. The metal support/anode interface was found to be crack-free and well-bonded.

Funding: This research was funded by subsidies in the framework of the program to improve the competitiveness of TPU and Project VIU_NU_187_2014.

References

- [1] M.C. Tucker, *J. Power Sources*, 195 (2010) 4570–4582.
- [2] J.H. Lee, H. Moon, H.W. Lee, J. Kim, J.D. Kim and K.H. Yoon, *Solid State Ionics*, 148 (2002) 15–26.
- [3] P. Gannon, S. Sofie, M. Deibert, R. Smith and V. Gorokhovskiy, *J. Appl. Electrochem.*, 39 (2009) 497–502.
- [4] D. Lee, D. Kim and J. Kim, *J. Moon, Sci. Rep.*, 4 (2014) 3937.
- [5] S. Kim, O. Kwon, S. Kumar, Y. Xiong and C. Lee, *Surf. Coatings Technol.*, 202 (2008) 3180–3186.
- [6] A.A. Solov'yev, N.S. Sochugov, S.V. Rabotkin, A.V. Shipilova, I.V. Ionov, A.N. Kovalchuk and A.O. Borduleva, *Appl. Surf. Sci.*, 310 (2014) 272–277.
- [7] H.S. Noh, J.W. Son, H. Lee, H. Ji, J.H. Lee and H.W. Lee, *J. Eur. Ceram. Soc.*, 30 (2010) 3415–3423.
- [8] S.P. Jiang, *J. Electrochem. Soc.*, 150 (2003) E548–E559.
- [9] S.P. Jiang and S.H. Chan, *J. Mater. Sci.*, 39 (2004) 4405–4439.
- [10] G. Schiller, T. Franco, M. Lang, P. Metzger and A.O. Stormer, *Electrochem. Soc. Proc.*, 07 (2005) 66–75.
- [11] D. Stöver, D. Hathiramani, R. Vaßen and R.J. Damani, *Surf. Coat. Technol.*, 201 (2006) 2002–2005.
- [12] Y.B. Matus, L.C.D. Jonghe, C.P. Jacobson and S.J. Visco, *Solid State Ionics*, 176 (2005) 443–449.
- [13] X.J. Chen, K.A. Khor, S.H. Chan and L.G. Yu, *Mater. Sci. Eng. A*, 341 (2003) 43–48.
- [14] K. Rajeswari, U.S. Hareesh, R. Subasri, D. Chakravarty and R. Johnson, *Sci. Sinter*, 42 (2010) 259–267.
- [15] K. Rajeswari, M.B. Suresh, D. Chakravarty, D. Das and R. Johnson, *Int. J. Hydrogen Energy*, 37 (2012) 511–517.
- [16] X. Weng, D. Brett, V. Yufit, P. Shearing, N. Brandon, M. Reece, H. Yan, C. Tighe and J.A. Darr, *Solid State Ionics*, 181 (2010) 827–834.
- [17] J.Y. Yoo, I.J. Shon, B.H. Choi and K.T. Lee, *Ceram. Int.*, 37 (2011) 2569–2574.
- [18] A.I. Kiryashkin, V.D. Kitler, A.S. Maznoy, A.A. Solov'ev, A.N. Kovalchuk and I.V. Ionov, *Adv. Materials Res.*, 1040 (2014) 19–23.
- [19] A.A. Shchepetkin and G.I. Chufarov, *Russ. J. Inorg. Chem.*, 17 (1972) 792–794.
- [20] O. Bezdorozhev, H. Borodianska, Y. Sakka and O. Vasylykiv, *J. Nanosci. Nanotechnol.*, 13 (2013) 4150–4157.
- [21] O. Bezdorozhev, H. Borodianska, Y. Sakka and O. Vasylykiv, *J. Nanosci. Nanotechnol.*, 14 (2014) 4218–4223.